A Robust Watermarking Against Shearing Based on Improved S-Radon Transformation

Deng Minghui[1,2]
[1]School of Astronautics, Harbin Institute of Technology
[2]Department of Engineering, Northeast Agricultural University, Harbin, China
Email: markdmh@163.com

Zeng Qingshuang*
School of Astronautics, Harbin Institute of Technology
Harbin, China
Email: zqshuang2000@yahoo.com.cn

Zhou Xiuli
Department of Engineering, Northeast Agricultural University
Harbin, China
Email: zhouxiuli@neau.edu.cn

***Abstract*—In this paper, a robust image watermarking method in two-dimensional space/spatial-frequency distributions domain is proposed which is robust against geometric distortion. This watermarking is detected by a linear frequency change. The one-dimensional S transformation and radon transformation are used to detect the watermark. The chirp signals are used as watermarks and this type of signals is resistant to all stationary filtering methods and exhibits geometrical symmetry. In the two-dimensional Radon-Wigner transformation domain, the chirp signals used as watermarks change only its position in space/spatial-frequency distribution, after applying linear geometrical attack, such as scale rotation and cropping. But the two-dimensional Radon-Wigner transformation needs too much difficult computing. So the image is put into a series of 1D signal by choosing scalable local time windows. The watermark embedded in the 1D improved S-Radon transformation domains. The watermark thus generated is invisible and performs well in StirMark test and is robust to geometrical attacks. Compared with other watermarking algorithms, this algorithm is more robust, especially against geometric distortion, while having excellent frequency properties.**

***Index Terms*—Digital watermarking, improved S-Radon transform, Geometrical attack**

I. INTRODUCTION

With the arrival of the information era and the broad application of E-business, there is a growing importance to protect the security of messages. As an important branch in the field of the research on the message cryptic technique, the digital watermarking technique is an efficient way to the authentication of content and copyright. This technique authenticate and protect the data by imbed watermark in the original data. The watermark imbedded can be a passage, some marks or images. The traditional encryption can only assure the message security when being visited and the security of both parts when in a single-phase communication mode, but to the public messages transformed in the multi phase mode a new technique and mechanism is needed. As a potential method to solve the problem, digital watermarking technique is being widely concerned, and it is becoming the top research in the international academic field.

Digital watermark is a special mark cryptic in the multi-media products. Digital watermark should have three basic characteristics: Insensitive, that is the imbed watermark can't destroy the digital products, and we can feel the exist of the watermark neither visual nor aural; robustness, that is under the usual signal processing (compressed, rejected or effected by noise) and geometric transmitting (translated, flexed or rotated), It can assure that the watermark can't be destroyed. The imbedded watermark can be done in time-space frequency, and it can also be done in the transformable domain. The first method is easy to be carried out, but the protecting from the attack to signal processing can't be done perfectly. However, the watermarking method under transformable domain is better. The robustness must be better in the efficient digital watermark in [1]-[7].

In this paper we put forward a robust digital image watermarking based on S-Radon transform. In Srdjan Stankovic's paper, a watermarking algorithm in the space/spatial domain using two-dimensional Radon-Wigner distribution is introduced. This algorithm uses of the Radon-Wigner transform to detect the watermark and the two-dimensional chirp signals are used as watermarks. In the two-dimensional Radon-Wigner transformation domain, the chirp signals used as watermarks change only its position in space/spatial-frequency distribution, after applying linear geometrical attack, such as scale rotation

doi:10.4304/jcp.7.10.2549-2556

and cropping. Compared with other watermarking algorithms, this algorithm is more robust, especially against geometric distortion, while having excellent frequency properties. But the 2D Radon-Wigner transformation needs much difficult computing and can be impossible in reality. So we introduce a algorithm based on 1D S transform. In this algorithm, the chirp signals used as watermarks are inserted in the image and the image is put into a series of 1D signal by choosing scalable local time windows. By using improved S-Radon transformation on the 1D image signal series, the watermark is detected. The shearing attack can break watermarks in one part of space support district, but watermarks in another one part of space support district still can not be destroyed. Synthesizing each supporting space, the watermark extracted still can be clear and the algorithm achieves the robustness to the shearing attacks.

II. THE PRINCIPLE OF S TRANSFORM

As a linear time-frequency analysis, S transform in [8] has some features similar to the nature of time-frequency domain of the Fourier transform and the wavelet transform. For example, it is a reversible transformation of non-destructive and it's inverse transform can perfectly reconstruct the original signal. So the time-frequency invariant feature ensures that the invariant features with the transformation signal for a specific application. One-dimensional S transform is:

$$S(\tau, f)=\int_{-\infty}^{+\infty} h(t)\frac{|f|}{\sqrt{2\pi}}e^{\frac{-(t-\tau)^2 f^2}{2}}e^{-i2\pi ft}dt \tag{1}$$

where t, r are t domain variables and f is frequency domain variable. One-dimensional signal $h(t)$ is mapped from the one-dimensional time domain to the two-dimensional time-frequency plane through S transform. One-dimensional S inverse transform is

$$h(t)=\int_{-\infty}^{+\infty}\int_{-\infty}^{+\infty} S(\tau, f)d\tau e^{i2\pi ft}df \tag{2}$$

If S transform is local spectrum, the Fourier spectrum can be received by computing the average local spectrum through the whole time domain. So S transformation:

$$\int_{-\infty}^{+\infty} S(\tau, f)d\tau = H(f) \tag{3}$$

$H(f)$ is the Fourier transform of $h(t)$. $h(t)$ can be deduced from $S(\tau, f)$. S transform is the general Fourier transform of non-stationary time series.

S transform is the linear computation of time series $h(t)$. The transformed noise can often influence time-frequency resolution ratio. If signal $x(t)$ is equal to the sum of original data $s(t)$ and noise $n(t)$.

$$x(t)=s(t)+n(t) \tag{4}$$

After S transform:

$$S\{x(t)\}=S\{s(t)\}+S\{n(t)\} \tag{5}$$

The S transform can not creat cross terms and overwhelmingly increase the time-frequency resolution ratio. If the S transform of $h(t)$ is $S(\tau, f)$, the S transform of $h(t-r)$ is $S(\tau-r, f)e^{-i2\pi fr}$.

From equation 3, we can know that S transform has direct connection with Fourier transform. S transform and S inverse transform are a lossless reversible procedure. S transform will not create the cross terms and has nice time-frequency energy centralization quality.

Two-dimensional S transform is based on one-dimensional S transform to develop, that formula to transform is:

$$S(x,y,k_x,k_y)=\int_{-\infty}^{+\infty}\left[\int_{-\infty}^{+\infty} h(x',y')\frac{|k_x|}{\sqrt{2\pi}}e^{(x'-x)^2/2}e^{-i2\pi k_x x'}dx'\right]\frac{|k_y|}{\sqrt{2\pi}}e^{(y'-y)^2/2}e^{-i2\pi k_y y'}dy' \tag{6}$$

where $h(x', y')$ is the two-dimensional image and (x', y') is the space domain variables. After transformation, S transform spectrum contains 4 variables (x, y, k_x, k_y). (x, y) are the variables in space domain and (k_x, k_y) are the variables in frequency domain, also known as the wavelength. Similar to the two-dimensional Fourier transform, the nature of the two-dimensional S transform can be seen as a cascade of two one-dimensional S transformations.

Reference to the fast Fourier transform, the $h(n)(n=0,1,\mathrm{L}\ ,N)$ is the corresponding $h(t)$ discrete time series and sampling time interval is T. The discrete Fourier transform is:

$$H(\frac{1}{NT})=\frac{1}{N}\sum_{k=0}^{N-1}h(kT)e^{\frac{i2\pi nk}{N}} \tag{7}$$

The discrete S transformation of time series $h(t)$ is as follows:

$$S[jT,\frac{n}{NT}]=\sum_{m=0}^{N-1}H[\frac{m+n}{NT}]e^{\frac{2\pi^2m^2}{n^2}}e^{\frac{i2\pi mj}{N}} \tag{8}$$

When n = 0 (equivalent to zero frequency), discrete form of expression is:

$$S[jT,0]=\frac{1}{N}\sum_{m=0}^{N-1}h[\frac{m}{NT}] \tag{9}$$

Equ.9 ensures that the time series of anti-transformation can be accurate. Of course, discrete S transformation has been limited by sampling and the length and will have a border effect in time and frequency domain.

Discrete S inverse transformation is to obtain by calculating the discrete Fourier transform. When n is not equal to 0, the summation of S matrix (S [n, m]) along the line is:

$$S[jT,\frac{n}{NT}]=\sum_{j=0}^{N-1}\sum_{m=0}^{N-1}H[\frac{m+n}{NT}]e^{\frac{2\pi^2m^2}{n^2}}e^{\frac{i2\pi mj}{N}} \tag{10}$$

Equ.10 can be turned into:

$$S[jT,\frac{n}{NT}]=\sum_{m=0}^{N-1}H[\frac{m+n}{NT}]e^{\frac{2\pi^2m^2}{n^2}}\sum_{j=0}^{N-1}e^{\frac{i2\pi mj}{N}} \quad (11)$$

The average of $S[jT,\frac{n}{NT}]$ is:

$$S[jT,\frac{n}{NT}]=\sum_{m=0}^{N-1}N\delta_{m,0}H[\frac{m+n}{NT}]e^{\frac{2\pi^2m^2}{n^2}} \quad (12)$$

$$\frac{1}{N}S[jT,\frac{n}{NT}]=H[\frac{n}{NT}] \quad (13)$$

Therefore, discrete inverse S transformation is:

$$h[kT]=\frac{1}{N}\sum_{n=0}^{N-1}\left\{\sum_{j=0}^{N-1}S[\frac{n}{NT},jT]\right\}e^{\frac{i2\pi nj}{N}} \quad (14)$$

When n is equal to zero, the width of the Gaussian function is zero. Zero frequency is the average of time series and is constant. $S[jT,\frac{n}{NT}]$ is the average of $h[kT]$ when the value of n reduced to zero. That is, every value along zero n value is replaced by this value. In this way, it ensures that S transformation is completely reversible.

The generalized S-transform is given by

$$S(\tau,f,\beta)=\int_{-\infty}^{+\infty}h(t)\omega(\tau-t,f,\beta)e^{-i2\pi ft}dt \quad (15)$$

where ω is the window function of the S-transform and β denotes the set of parameters that determine the shape and property of the window function. The window satisfies the normalized condition

$$\int_{-\infty}^{+\infty}\omega(t,f,\beta)dt=1 \quad (16)$$

The alternative expression of (15) by using the convolution theorem through the Fourier transform can be written as

$$S(\tau,f,\beta)=\int_{-\infty}^{+\infty}X(\alpha+f)W(\alpha,f,\beta)e^{j2\pi\alpha\tau t}d\alpha \quad (17)$$

Where:

$$X(\alpha+f)=\int_{-\infty}^{+\infty}h(t)e^{-i2\pi(\alpha+f)t}dt \quad (18)$$

And

$$W(\alpha,f,\beta)=\int_{-\infty}^{+\infty}\omega(t,f,\beta)e^{-i2\pi\alpha t}dt \quad (19)$$

The variable α and f in the above expression have the same units. In this scheme we retain the window function as the same Gaussian window because it satisfies the minimum value of the uncertainty principle. We have introduced an additional parameter (into the Gaussian window where its width varies with frequency as follows

$$\sigma(f)=\frac{\delta}{|f|} \quad (20)$$

Hence the generalized S-transform becomes

$$S(\tau,f,\delta)=\int_{-\infty}^{+\infty}h(t)\frac{|f|}{\sqrt{2\pi}\delta}e^{\frac{-(\tau-t)^2f^2}{2\delta^2}}e^{-i2\pi ft}dt \quad (21)$$

Where the Gaussian window becomes

$$\omega(t,f,\delta)=\frac{|f|}{\sqrt{2\pi}\delta}e^{\frac{-t^2f^2}{2\delta^2}} \quad (22)$$

And its frequency domain representation is

$$W(\alpha,f,\delta)=e^{-\frac{2\pi^2\sigma^2\delta^2}{f^2}} \quad (23)$$

III THE PRINCIPLE OF RADON TRANSFORM

The 2D Radon transformation is the projection of the image intensity along a radial line oriented at a specific angle [9]. Radon expresses the fact that reconstructing an image, using projections obtained by rotational scanning is feasible. His theorem is the following: The value of a 2-D function at an arbitrary point is uniquely obtained by the integrals along the lines of all directions passing the point. The Radon transformation shows the relationship between the 2-D object and its projections [10].

The Radon Transformation is a fundamental tool which is used in various applications such as radar imaging, geophysical imaging, nondestructive testing and medical imaging [11]. Many publications exploit the Radon Transformation. Meneses-Fabian et al. [12] describe a novel technique for obtaining border-enhanced topographic images of a slice belonging to a phase object. Vítezslav [13] examines fast implementations of the inverse Radon transform for filtered back projection on computer graphic cards. Sandberg et al. [14] describe a novel algorithm for topographic reconstruction of 3-D biological data obtained by a transmission electron microscope. Milanfar [15] exploits the shift property of Radon transformation to image processing. Barva et al. [16] present a method for automatic electrode localization in soft tissue from radio-frequency signal, by exploiting a property of the Radon Transform. Challenor et al. [17] generalize the two dimensional Radon transform to three dimensions and use it to study atmospheric and ocean dynamics phenomena.

Figure 2 illustrates several 1D projections from different angles of an image consisting of three spots in the 2D domain. In some of the projections, only two spots are shown. This reveals the importance of the selection of the "correct" projections for image reconstruction.

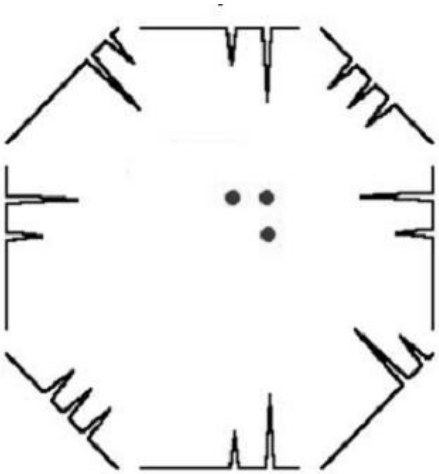

Figure1. Different projections of a three-dot image example

Suppose a 2-D function $f(x,y)$ (Fig. 3). Integrating along the line, whose normal vector is in θ direction, results in the $g(s,\theta)$ function which is the projection of the 2D function $f(x,y)$ on the axis s of θ direction. When s is zero, the g function has the value $g(0,\theta)$ which is obtained by the integration along the line passing the origin of (x,y) -coordinate. The points on the line whose normal vector is in θ direction and passes the origin of (x,y) -coordinate satisfy the equation:

$$\frac{y}{x}=\tan(\theta+\frac{\pi}{2})=\frac{-\cos\theta}{\sin\theta} \quad \Rightarrow$$
$$\Rightarrow \quad x\cos\theta+y\sin\theta=0$$

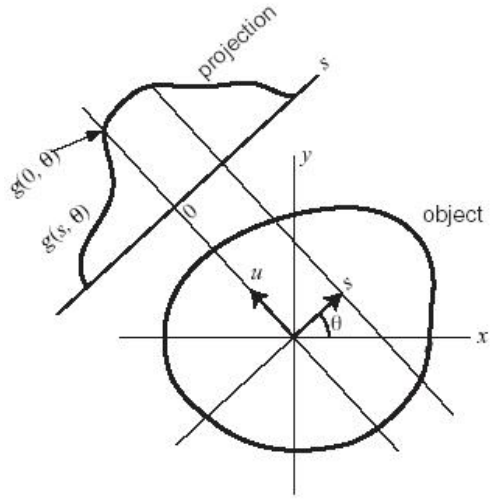

Figure2. The Radon Transform computation

The integration along the line whose normal vector is in θ direction and that passes the origin of (x,y) -coordinate means the integration of $f(x,y)$ only at the points satisfying the previous equation. With the help of the Dirac "function" δ , which is zero for every argument except to 0 and its integral is one, $g(0,\theta)$ is expressed as:

$$g(0,\theta)=\iint f(x,y)\cdot\delta(x\cos\theta+y\sin\theta)\,dxdy \qquad (24)$$

Similarly, the line with normal vector in θ direction and distance s from the origin is satisfying the following equation:

$$(x-s\cdot\cos\theta)\cdot\cos\theta+(y-s\cdot\sin\theta)\cdot\sin\theta=0 \quad \Rightarrow$$
$$x\cos\theta+y\sin\theta-s=0$$

So the general equation of the Radon transformation is acquired: [10, 11, 15, 16, 18]

$$g(s,\theta)=\iint f(x,y)\cdot\delta(x\cos\theta+y\sin\theta-s)\,dxdy \qquad (25)$$

The inverse of Radon transform is calculated by the following equation [14] :

$$f(x,y)=\int_{-\pi/2}^{\pi/2}\rho\cdot R_\theta\big(s(x,y)\big)\,d\theta \qquad (26)$$

where R_θ is the Radon transformation, ρ is a filter and

$$s(x,y)=x\cos\theta+y\sin\theta \qquad (27)$$

Radon-Wigner transformation is a kind of projective transformation of linear integration, It is the Radon transformation of linear integration projection for the signal wigner transformation, as shown in the Figure3.

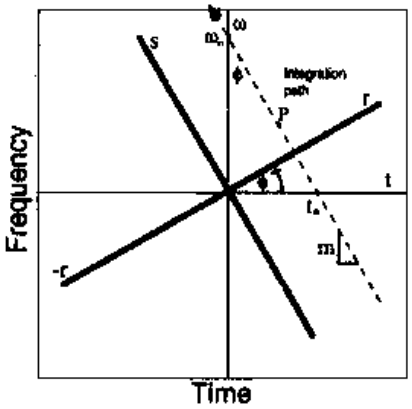

Ficture3. Schematic illustrating the geometry for calculation of the Radon-Wigner spectrum

The Wigner distribution of the image I (x, y) is defined as:

$$WD(x,y,\omega_x,\omega_y)$$
$$=\int_{-\infty}^{+\infty}\int_{-\infty}^{+\infty}I(x+\xi/2,y+\zeta/2)I^*(x-\xi/2,y-\zeta/2)$$
$$\times e^{-j(\omega_x\xi+\omega_y\zeta)}d\xi d\zeta$$

its pseudo form is used in practical realizations

$$WD(x,y,\omega_x,\omega_y)$$
$$=\int_{-\infty}^{+\infty}\int_{-\infty}^{+\infty}I(x+\xi/2,y+\zeta/2)I^*(x-\xi/2,y-\zeta/2)$$
$$\times w(\xi,\zeta)\;\; w^*(-\xi,-\zeta)e^{-j(\omega_x\xi+\omega_y\zeta)}d\xi d\zeta$$

where $w(\xi,\zeta)$ is a 2D window function. The 2D chirp signal, used here as a base for watermarking, has this form:

$$\Omega(x,y) = 2A\cos(ax^2+by^2+c) = A(e^{j(ax^2+by^2+c)} + e^{-j(ax^2+by^2+c)})$$

where A is the watermark amplitude or strength. Note that the Wigner distribution of this signal is highly concentrated.

$$WD(x,y,\omega_x,\omega_y) = A^2W(\omega_x-2ax,\omega_y-2by) + A^2W(\omega_x+2ax,\omega_y+2by) + cross-terms$$

where the Fourier transform of the window. $w(\omega_x-2ax,\omega_y-2by)$, is close to a delta function $\delta(\omega_x-2ax,\omega_y-2by)$ for a sufficiently wide window, since the cross-terms in the Wigner distribution will be eliminated by use of projections, they will be neglected in the sequel.

After a general linear geometrical transformation, signal can be written in this form

$$\Omega'(x,y) = 2A\cos(a_1x^2+a_2y^2+a_3xy+a_4x+a_5y+a_6)$$

This transformation corresponds to a mapping of centered ellipse into the rotated one, whose center is displaced from the origin. From the point of view of the Wigner distribution concentration on the local frequency, we may say that it is invariant with respect to this transformation. Only the position of the local frequency of the distribution concentration will be changed.

$$WD(x,y,\omega_x,\omega_y) = A^2W(\omega_x-2a_1x-a_3y-ax, \omega_y-2a_2y-a_3x-a_5) + A^2W(\omega_x+2a_1x+a_3y+ax, \omega_y+2a_2y+a_3x+a_5) + cross-terms$$

This means that the described geometrical transformation does not influence the maximal value of the Wigner distribution which we intend to use for the watermark detection. The Wigner distribution of the watermark remains close to the delta pulse. Although, we have a very specific and recognizable function over the enter space, its energy could be much smaller than the energy of the Wigner distribution of an image because the value of A should be drastically smeller than the average image values. For this reason the watermark detection of us only the Wigner distribution is not reliable enough.

IV. THE IMBEDDING AND TEST OF DIGITAL WATERMARK

We consider how to construct a watermark to insert into the image. In the Srdjan Stankovic and Igor Djurovic's paper, the two-dimensional chirp signals are used as watermarks and in the algorithm two-dimensional Radon-Wigner transformation is applied to additionally concentrate the energy of the watermark signal and shows perfect robustness to the geometrical attacks. But the computing of two-dimensional Radon-Wigner needs too much time and could be very difficult. This algorithm is very impractical and the ordinary computer could not finish this work. So we want to look for a new time – frequency distributions domain algorithm to solve this problem.

We imbed the watermark in the S transformation domain of image. In Stockwell's paper, the S transformation is introduced and can detect linear frequency-modulated signals. But 2D S transformation needs expensive computing. Obviously, it is necessary to apply one-dimensional S transformation on image and additionally concentrate the energy of the watermark signals. We select the linear frequency-modulated signals as watermark. The digital watermark is W with the sum of many linear frequency-modulated signals with different frequency:

$$W(n)=\cos[2\pi(f_1+k_1nT)nT]+L+\cos[2\pi(f_m+k_mnT)nT] \quad (28)$$

The length of W is n, and then choose D0 and D1 two areas with the same size of watermark in wavelet transformation middle frequency domain LH_0 and HL_0 of digital image frame C_{ij}. The method to imbed watermark is as followed:

$$D_0'(i,j)=(D_0(i,j)+W(n)), D_1'(i,j)=(D_1(i,j)+W(n)) \quad (29)$$

Then we synthesize wavelet to get watermark image. All the frames be done the same way as above-mentioned calculate ways. When withdrawing watermark, we carry on wavelet decomposition again and withdraw a 1-D signal from the known domains. We make S transformation on the 1-D signal and detect the linear frequency-modulated signals that are the watermarks. Then we take Radon transformation on the S transformation image and the more clear watermarks is shown.

In this paper, we use standard 256 ×256 gray image Lena as an original image. Applying Haar wavelet transformation in the algorithm, the image after imbedded the two and three linear frequency-modulated signals with different frequency as watermark is shown in Ficture4. The detecting result is shown in Ficture5 and Ficture6. The picture frame decomposition adding three watermarks cuts pictures in the different position and the different size. After cutting an attack withdraw watermark. We cut 50% and 75% of the image random such as Ficture7 Ficture12. Then extracted watermark result is shown such as follows. According to the result of the experiment, it can be seen that the watermarking image can still be extracted well even the original image is shearing attacked by 75% with the S-Radon transformation. This algorithm is better than the S transformation and Wigner transformation. This proves the efficient of the method used above. In the testing process, this algorithm can be used in the reality.

Ficture4.Watermarked image

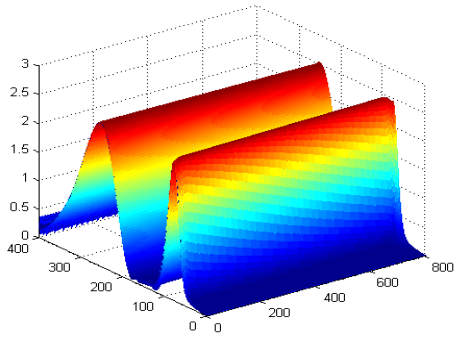

Ficture5. The two Watermarks extracted with S transformation

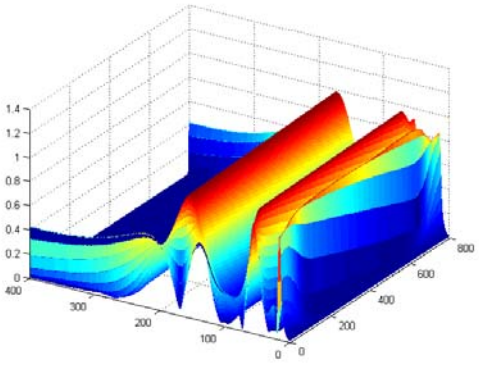

Ficture6. The three Watermarks extracted with S transformation

Ficture7.Sheared by 50% in the middle

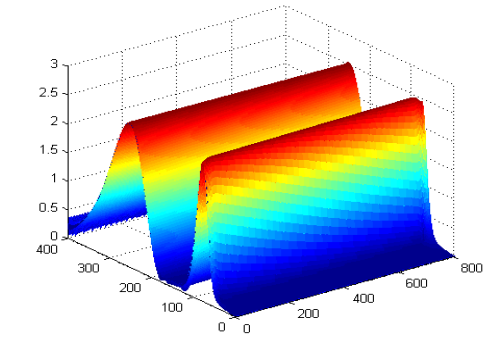

Ficture8. The two Watermarks extracted with S transformation

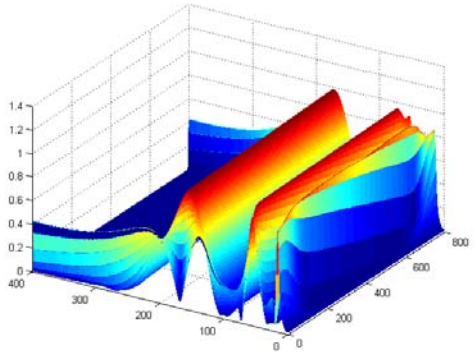

Ficture9. The three Watermarks extracted with S transformation

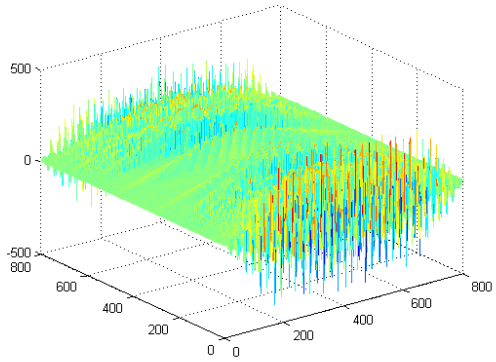

Ficture10. The three Watermarks extracted with Wigner transformation

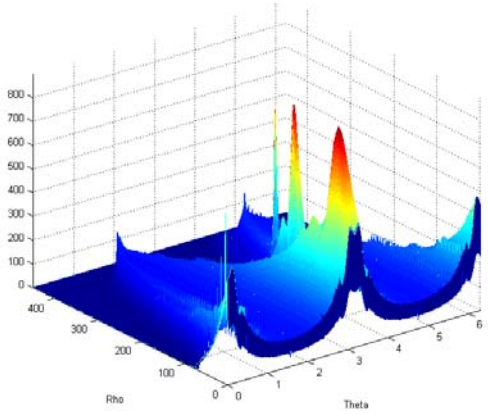

Ficture11. The three Watermarks extracted with improved S-Radon transformation

Ficture12. Sheared by 75% upside

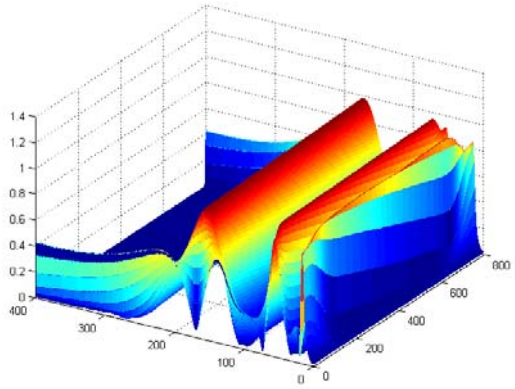

Ficture13. The three Watermarks extracted with S transformation

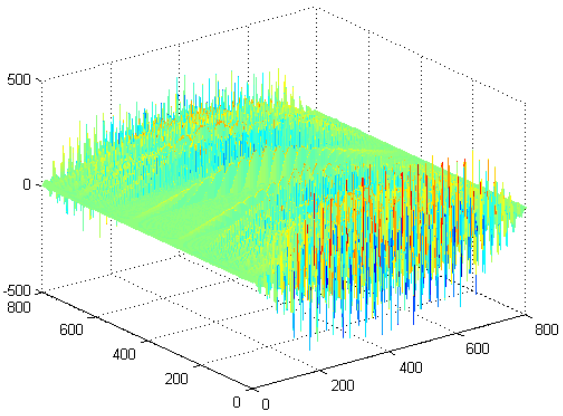

Ficture14. The three Watermarks extracted with Wigner transformation

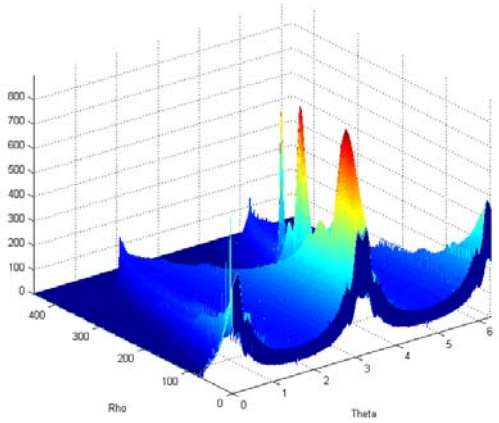

Ficture15. The three Watermarks extracted with improved S-Radon transformation

V. CONCLUSIONS

In this paper, a robust watermarking method against shearing based on S-Radon transform is introduced. The proposed method makes use of the person's sense of vision characteristics and wavelet transformation to achieve the improved S-Radon transform on the image. The linear frequency-modulated signals are selected as watermarks and are added in middle frequency coefficients in the transformation matrix. Based on 1D S transform and Radon transformation, the watermark is extracted. The method improves the validity of watermarking and shows excellent advantage against shearing attack.

ACKNOWLEDGMENT

This paper is supported by the 2009 Natural Science Program of Heilongjiang Province Educational Committee (NO.11541016) and the Doctor Startup Funding of Northeast Agricultural University

REFERENCES

[1] RUANAIDH J J K, PUN T. Rotation, scale and translation spread spectrum digital image watermarking [J]. Signal Processing, 1998, 66(3): 303~317.

[2] SRDJAN STANKOVIC, IGOR DJUROVIC, IOANNIS PITAS. Watermarking in the space/spatial-frequency domain using two-dimensional radon-wigner distribution [J]. IEEE Transactions on Image Processing. 2001, 10(4): 650-658.

[3] COX I J, KILIAN J, LEIGHTON F T. Secure Spread Spectrum Watermarking For Multimedia [J]. IEEE Tran. of Image Processing ,1997,6(12),1673~1687.

[4] LINNARTZ J P, DEPOVERE G, and KALKER T. On the Design of a Watermarking system: Considerations and Rationales [A]. In: Information hiding Third International Workshop, IH'99, Dresden, Germany. (1999), 253~269.

[5] R G VAN SCHYNDEL, A Z TIRKEL, CF OSBORNE. [A]. In: Proceeding of IEEE International Conference on Image Processing [C], Vancouver, Canada 1994,2:86~94.

[6] NIV Xia–mu, LU Zhe–ming, SVN Sheng–he. Digital watermarking of still image with gray –level digital watermarks [J]. IEEE Trans .On Consumer Electronics, 2000,46(1), 137~239.

[7] Huang Ji-wu, Tan Tie-niu. Summary of the Image In plate Watermark [J]. Electronic Paper, 2000, 26(5): 645~655.
[8] STORCKWELL R G, MANSINHA L, LOWE R P, Localization of the Complex Spectrum: The S-Transform. IEEE Transactions on Signal Processnig, 1996, 44(4): 998-1001.
[9] . Mathworks,http://www.mathworks.com, accessed 15 June 2005.
[10] A. Asano, "Radon transformation and projection theorem", Topic 5, Lecture notes of subject Pattern information processing, 2002 Autumn Semester, http://kuva.mis.hiroshima-u.ac.jp/~asano/Kougi/02a/PIP/
[11] A. Averbuch, R.R. Coifman, D.L. Donoho, M. Israeli, J. Wald´en, Fast Slant Stack: A notion of Radon Transform for Data in a Cartesian Grid which is Rapidly Computible, Algebraically Exact, Geometrically Faithful and Invertible., to appear in SIAM J. Scientific. Computing, 2001
[12] C. Meneses-Fabian, G. Rodr´ýguez-Zurita, and J.F. V´azquez-Castillo "Optical tomography of phase objects with parallel projection differences and ESPI", Investigacion revista mexicana de fisica 49 (3) 251–257 Junio 2003.
[13] V.V. Vlcek, "Computation of Inverse Radon Transform on Graphics Cards", International Journal of Signal Processing 1(1) 2004 1-12.
[14] K. Sandberg, D. N. Mastronarde, G. Beylkina, "A fast reconstruction algorithm for electron microscope tomography", Journal of Structural Biology 144 (2003) 61–72, 3 September 2003.
[15] P. Milanfar, "A Model of the Effect of Image Motion in the Radon Transform Domain", IEEE Transactions on Image processing, vol. 8, no. 9, September 1999
[16] M. Barva and J. Kybic with J. Mari and C. Cachard, "Radial Radon Transform dedicated to Micro-object Localization from Radio Frequency Ultrasound Signal", In UFFC '04: Proceedings of the IEEE International Ultrasonics, Ferroelectrics and Conference. Piscataway: IEEE, 2004, p. 1836-1839. ISBN 0-7803-8412-1.
[17] P.G. Challenor , P. Cipollini and D. Cromwell, "Use of the 3D Radon Transform to Examine the Properties of Oceanic Rossby Waves", Journal of Atmospheric and Oceanic Technology, Volume 18, 22 January 2001.

Deng Minghui was born 1976 in Harbin China. He received the B.S. degree in application of electronic technology from Harbin Engineering University in 1999 and the M.S. degree in mode distinguishing and brainpower system from Harbin Engineering University in 2002 and the Ph.D. degree in control theory and control engineering from Harbin Engineering University in 2005.

From 2005 to 2006, he worked in Heilongjiang University as a lecturer. Since 2007 he has been a vice professor in Northeast Agricultural University. In 2010 he made postdoctoral study in Harbin Institute of Technology.

Dr. Deng is working in image watermarking and information security.

Zeng Qingshuang was born 1965 in Harbin China. He received the B.S. degree in automatic control from Harbin Institute of Technology in 1987, the M.S. degree in control theory and applications from Harbin Institute of Technology in 1990 and the Ph.D. degree in navigation, guidance and control from Harbin Institute of Technology in 1997.

Dr. Zeng is working in Navigation and Control Theory as a professor in Harbin Institute of Technology.

Zhou Xiuli was born 1966 in Hegang China. He received the B.S. degree in Electrical Engineering from Northeast Agricultural University in 1986, the M.S. degree in control theory and control engineering from Northeast Agricultural University in 1992. Dr. Zeng is working in Information Processing and Control Theory as a professor in Northeast Agricultural University.